Title

Bacteria engineered to produce IL-22 in intestine induce expression of REG3G to reduce ethanol-induced liver disease in mice

Journal

Gut, 68(8)

ISSN

0017-5749

Authors

Hendrikx, Tim
Duan, Yi
Wang, Yanhan
et al.

Publication Date

2019-08-01

DOI

10.1136/gutjnl-2018-317232

Peer reviewed

Gut. Author manuscript; available in PMC 2020 May 17.

Bacteria Engineered to Produce IL22 in Intestine Induce Expression of REG3G to Reduce Ethanol-induced Liver Disease in Mice

Tim Hendrikx[1], **Yi Duan**[1,2], **Yanhan Wang**[1,2], **Jee-Hwan Oh**[3], **Laura M. Alexander**[3], **Wendy Huang**[4], **Peter Stärkel**[5], **Samuel B. Ho**[1,2], **Bei Gao**[6], **Oliver Fiehn**[6], **Patrick Emond**[7,8], **Harry Sokol**[9,10,11], **Jan-Peter van Pijkeren**[3], and **Bernd Schnabl**[1,2]

[1]Department of Medicine, University of California San Diego, La Jolla, California

[2]Department of Medicine, VA San Diego Healthcare System, San Diego, California

[3]Department of Food Science, University of Wisconsin-Madison, Madison, Wisconsin

[4]Department of Cellular and Molecular Medicine, University of California San Diego, La Jolla, California

[5]Laboratory of Hepato-Gastroenterology, Institute of Experimental and Clinical Research, Université catholique de Louvain, Brussels, Belgium

[6]West Coast Metabolomics Center, University of California, Davis, CA, USA

[7]UMR 1253, iBrain, Université de Tours, Inserm, France

[8]CHRU de Tours, Service de Médecine Nucléaire In Vitro, Tours, France

[9]Sorbonne Universités, UPMC Univ. Paris 06, École normale supérieure, CNRS, INSERM, APHP Laboratoire des Biomolécules (LBM), Paris, France

[10]Micalis Institute, Institut National de la Recherche Agronomique (INRA), AgroParisTech, Université Paris–Saclay, Jouy-en-Josas, France

[11]Department of Gastroenterology, Saint Antoine Hospital, Assistance Publique–Hopitaux de Paris, Paris, France

Abstract

Objective—Antimicrobial C-type lectin regenerating islet-derived 3 gamma (REG3G) is suppressed in the small intestine during chronic ethanol feeding. Our aim was to determine the mechanism that underlies REG3G suppression during experimental alcoholic liver disease.

Corresponding author: Bernd Schnabl, MD, Dept. of Medicine, University of California San Diego, Tel.: 0018588225311, beschnabl@ucsd.edu.

Author Contributions

TH designed and performed the experiments, analyzed and interpreted the data and wrote the manuscript; YD, YW provided technical support and critically revised the manuscript. JHO, LMA, PS, SH, BG, OF, HS, JPvP provided technical and material support and critically revised the manuscript. BS conceived, designed, and supervised the study, wrote and critically revised the manuscript.

Declaration of Interest

The authors declare no competing interests.

Design—Interleukin 22 (IL22) regulates expression of REG3G. Therefore, we investigated the role of IL22 in mice subjected to chronic-binge ethanol feeding (NIAAA model).

Results—In a mouse model of alcoholic liver disease, we found that type 3 innate lymphoid cells produce lower levels of IL22. Reduced IL22 production was the result of ethanol-induced dysbiosis and lower intestinal levels of indole-3-acetic acid (IAA), a microbiota-derived ligand of the aryl hydrocarbon receptor (AHR), which regulates expression of IL22. Importantly, fecal levels of IAA were also found to be lower in patients with alcoholic hepatitis compared to healthy controls. Supplementation to restore intestinal levels of IAA protected mice from ethanol-induced steatohepatitis by inducing intestinal expression of IL22 and REG3G, which prevented translocation of bacteria to liver. We engineered *Lactobacillus reuteri* to produce IL22 (*L. reuteri*/IL22) and fed them to mice along with the ethanol diet; these mice had reduced liver damage, inflammation, and bacterial translocation to the liver compared to mice fed an isogenic control strain, and upregulated expression of REG3G in intestine. However, *L. reuteri*/IL22 did not reduce ethanol-induced liver disease in *Reg3g*$^{-/-}$ mice.

Conclusion—Ethanol-associated dysbiosis reduces levels of IAA and activation of the AHR to decrease expression of IL22 in the intestine, leading to reduced expression of REG3G—this results in bacterial translocation to the liver and steatohepatitis. Bacteria engineered to produce IL22 induce expression of REG3G to reduce ethanol-induced steatohepatitis.

Keywords

ILC; microbiome; metabolome; immune response

Introduction

Alcoholic liver disease affects several million people worldwide and can progress from hepatic steatosis and alcoholic steatohepatitis to cirrhosis and hepatocellular carcinoma [1]. In 2010, alcohol-attributable chronic liver disease was responsible for almost 500,000 deaths globally. Chronic alcohol intake contributes to gut barrier dysfunction, increased intestinal permeability, and changes in gut microbiota composition (dysbiosis) [2]. Moreover, transplantation of gut microbiota from patients with alcoholic hepatitis to mice demonstrated that alcohol-associated dysbiosis contributes to the development of severe liver disease and is transmissible, through fecal microbiota transfer [3].

C-type lectins mediate the intestinal immune response against pathogens and maintain homeostasis of commensal microbes [4]. One C-type lectin, regenerating family member 3 gamma (REG3G), is primarily expressed in the small intestine. Levels of REG3G are reduced in small intestines of mice after chronic ethanol feeding and in the duodenum of patients with alcohol use disorder [5, 6]. *Reg3g*$^{-/-}$ mice have increased susceptibility to ethanol-induced liver disease, in association with increased translocation of bacteria to the liver [7]. On the other hand, intestine-specific overexpression of REG3G protects mice against ethanol-induced liver disease by reducing bacterial translocation. However, the mechanism by which chronic ethanol feeding reduces intestinal expression of REG3G and increases bacterial translocation is unknown.

The production of REG3G lectins is regulated by interleukin 22 (IL22), a cytokine mainly expressed by RORγt^+ type 3 innate lymphoid cells (ILC3) in the gut during homeostasis [8]. Here, we investigated whether ethanol-induced dysbiosis impairs IL22 production in the gut and expression of REG3G to promote bacterial translocation and liver disease. We also tested the effects of IL22-producing bioengineered bacteria on ethanol-induced liver disease in mice.

Results

Chronic–binge ethanol feeding reduces intestinal production of IL22 by ILC3 in mice

Chronic alcohol feeding reduces intestinal levels of *Reg3g* mRNA and protein in mice and humans [5, 6]. We performed studies with chronic–binge ethanol-fed mice as a model of alcoholic steatohepatitis [9]. These mice had significant increases in mean plasma level of alanine aminotransferase (ALT) and hepatic level of triglycerides (Fig. 1a–c), and a reduced level of *Reg3g* and *Reg3b* mRNA in the small intestinal epithelium compared to pair-fed mice on an isocaloric diet (controls) (Fig.1d, e). The expression of other antimicrobial proteins Defensin alpha 3 (*Defcr3*), Defensin alpha 5 (*Defcr5*), *S100a8* and Lipocalin 2 (*Lcn2*) in the small intestine was not changed (See Supplementary 1 Fig. S1a). As the expression of *Reg3g* can be modulated via recognition of bacterial ligands by Toll-like receptor 4 (TLR4) [10] and subsequent MyD88 activation [11], *Tlr4* and *Myd88* mRNA levels were assessed in small intestinal epithelial cells. No difference was observed in the expression levels of *Tlr4* and *MyD88* between ethanol- and isocaloric-fed mice (See Supplementary 1 Fig. S1a). Yet, the ethanol-fed mice had a significant decrease in level of *Il22* mRNA in total lamina propria cells of the small intestine compared to controls (Fig. 1f). In addition, the frequency of IL22-expressing ILC3 (gated on CD3-RORγt^+) was significantly reduced in ethanol-fed mice compared to controls (Fig. 1g), while expression of the IL22 receptor subunit alpha 1 (*Il22Ra1*) in small intestinal epithelium did not differ (See Supplementary 1 Fig S1a). Further, increased expression of interleukin 1 beta (*Il1b*) and interleukin 18 (*Il18*) were found in small intestine of chronic-binge ethanol-fed mice compared to controls, while interleukin 10 (*Il10*), another IL10 family member, and interleukin 25 (*Il25*), which is able to repress IL22 production by RORγt^+ ILC3s [12, 13], did not change (See Supplementary 1 Fig. S1b).

To determine whether the reduction in IL22 expression is a direct effect of ethanol, we measured IL22 expression in lamina propria cells that were either pre-incubated for 1h or co-incubated for 4h with ethanol (50 mM or 100 mM) during IL23 stimulation. Levels of *Il22* mRNA and the frequency of $IL22^+$ ILC3 did not differ between cells incubated with ethanol or under control conditions (See Supplementary 1 Fig. S2a-d). These findings provide evidence that ethanol indirectly reduces IL22 expression by ILC3 in the gut, thereby reducing expression of REG3G and REG3B.

Intestinal levels of indole-3-acetic acid (IAA) are reduced during ethanol feeding in mice and in alcoholic hepatitis patients

Alterations in the gut microbiota composition and bacterial overgrowth (dysbiosis), intestinal barrier dysfunction, and bacterial translocation have been implicated in

development of alcoholic liver disease [9]. Microbiota can modulate IL22 production via production of metabolites from tryptophan catabolism, called indoles, which are ligands for the aryl-hydrocarbon receptor (AHR) [14]. In line with results from AHR-deficient mice [15], we observed reduced *Il22* expression in ILC3 upon incubation with an AHR inhibitor (CH223191), indicating that IL22 production by lamina propria cells in the small intestine requires AHR (Fig. 2a).

We therefore measured intestinal levels of metabolites described as potent activators of AHR in mice after chronic–binge ethanol feeding or the control diet using targeted metabolomics. Mice on the chronic–binge ethanol diet had lower mean amounts of indole-3-acetic acid (IAA) (Fig. 2b), a microbiota-dependent AHR ligand [16], and indole-3-sulfate (Fig. 2c) in the small intestine. Levels of other potential AHR ligands such as tryptamine (Fig. 2d), indole-3-aldehyde (Fig. 2e), indole-3-acetamide (Fig. 2f), a pre-cursor of IAA, and indole-3-lactic acid [17] (Fig. 2g) did not differ significantly between mice fed the ethanol vs the control diet. These data indicate that ethanol feeding reduces microbiota-dependent production of AHR ligands from tryptophan, which could be responsible for the reduced IL22 production.

To validate our findings in a clinical setting, levels of microbiota-dependent AHR ligands were determined in stool samples from alcoholic hepatitis patients (n=13) and healthy controls (n=17). Similar to our findings in mice, fecal levels of IAA were significantly reduced in patients with alcoholic hepatitis compared to controls (Fig. 2h). In addition, indole-3-lactic acid was lower in feces from alcoholic hepatitis patients (Fig 2i). This data supports that ethanol consumption alters tryptophan catabolism, thereby potentially affecting antimicrobial defense mechanisms by Reg3 lectins.

Supplementation with IAA reduces ethanol-induced steatohepatitis

Since intestinal IAA levels were reduced in both, alcoholic hepatitis patients and mice fed a chronic-binge ethanol diet, we aimed to restore intestinal levels of IAA by oral supplementation to mice. Daily oral administration of IAA (20 mM) during chronic–binge ethanol feeding decreased liver damage and steatosis, indicated by the significant reductions in plasma levels of ALT and hepatic levels of triglyceride (Fig. 3a–c), whereas liver to body weight ratio was unchanged (See Supplementary 1 Fig. S3a). IAA administration did not affect plasma levels of ethanol or hepatic expression of *Cyp2e1* and *Adh1* mRNAs, which regulate hepatic metabolism of ethanol (See Supplementary 1 Fig. S3b–d). Supplementation with IAA restored expression of *Il22* and *Reg3g* mRNAs in small intestine compared to control mice (Fig. 3d, e).

IAA supplementation prevented ethanol-induced translocation of bacteria to liver (Fig. 3f). Moreover, hepatic expression of genes regulated by AHR, *Cyp1a1* and *Cyp1b1*, did not change significantly during IAA supplementation, indicating no significant systemic effects of IAA on AHR signaling in liver (See Supplementary 1 Fig. S3e, f). So, defects in AHR-mediated expression of IL22, resulting from reduced production of IAA, contribute to ethanol-induced steatohepatitis.

Alcohol-associated dysbiosis decreases intestinal IL22 production

To test whether the microbiome is involved in reducing the expression of IL22, we analyzed production of IL22 by ILC3 in small intestinal lamina propria cells of mice given non-absorbable antibiotics, which prevent alcohol-associated intestinal bacterial overgrowth and dysbiosis [18, 19]. Importantly, the antibiotics used in our approach (Polymyxin B and Neomycin) predominantly target aerobic Gram-negative bacteria (so mostly *Enterobacteriaceae*), thereby not removing all bacterial strains [20].

In line with our previous findings [18, 19], administration of non-absorbable antibiotics prevented development of ethanol-induced steatohepatitis in mice, indicated by reduced mean plasma levels of ALT and hepatic levels of triglycerides (Fig. 4a–c), and restored liver to body weight ratio (See Supplementary 1 Fig. S4a). We found no changes in plasma levels of ethanol (See Supplementary 1 Fig. S4b) or hepatic expression of *Cyp2e1* or *Adh1* genes (See Supplementary 1 Fig. S4c, d). The prevention of liver damage by non-absorbable antibiotics was associated with restored expression of *Il22* mRNA in lamina propria cells and IL22 production by ILC3 upon IL23 stimulation (Fig. 4d, e). Mechanistically, we observed that antibiotics treatment was associated with increased intestinal levels of the AHR ligand indole-3-lactic acid [17], while indole-3-acetic acid and indole-3-aldehyde levels did not significantly change (See Supplementary 1 Fig. S4e-g). This data supports that impaired intestinal IL22 production results from ethanol-associated dysbiosis causing altered tryptophan catabolism and AHR ligand production.

Bacteria engineered to produce IL22 reduce ethanol-induced steatohepatitis and bacterial translocation

With an aim to restore intestinal expression of IL22 in our mouse model of alcoholic liver disease, we developed a strain of *Lactobacillus reuteri* that produces mouse IL22 (*L. reuteri*/IL22). IL22 was only present in supernatants of overnight cultures of the engineered *L. reuteri*/IL22 strain (See Supplementary 1 Fig. S5a). Mice were given daily phosphate-buffered saline (PBS, control), isogenic *L. reuteri* (bacteria control), or *L. reuteri*/IL22 (10^7 CFU/d) by oral gavage during 10 days of chronic–binge ethanol feeding. Daily administration was necessary, given that *L. reuteri* does not colonize mice (See Supplementary 1 Fig. S5b). Systemic IL22 administration to mice reduces ethanol-induced liver disease and acute ethanol-induced hepatotoxicity [21, 22]. We therefore titrated bacteria so that we would not observe increased systemic levels of IL22. Administration of *L. reuteri* or *L. reuteri*/IL22 to mice did not affect their levels of IL22 in the circulation, suggesting an intestine-restricted effect (Fig. 5a). However, administration of *L. reuteri*/IL22 significantly reduced steatohepatitis (Fig 5b–d) and decreased levels of *Cxcl1* and *Cxcl2* mRNAs, compared to controls (Fig. 5e, f). Liver to body weight ratio was unaffected by bacteria (See Supplementary 1 Fig. S5c).

To evaluate effects on ethanol metabolism, we measured plasma levels of ethanol and hepatic expression of *Cyp2e1* and *Adh1*. We found no differences among groups of mice, indicating that the protective effect of *L. reuteri*/IL22 is independent of changes in ethanol metabolism (See Supplementary 1 Fig. S5d–f). Compared to controls, we found *L. reuteri*/IL22 administration increased expression of *Reg3g* mRNA in the small intestine of ethanol-

fed mice (Fig. 5g). Although a trend towards an increase in *Reg3b* mRNA was observed in the small intestine of *L. reuteri*/IL22-treated mice, no significant difference was seen in the expression levels compared to controls (See Supplementary 1 Fig. S5g). Similarly, expression of *Defcr3* and *Defcr5* was unchanged (See Supplementary 1 Fig. S5g). *L. reuteri*/IL22 also significantly reduced bacterial translocation to the liver during chronic–binge ethanol feeding, compared with the bacteria control (Fig. 5h). Unaltered *Occludin* mRNA levels indicate no effect on tight junctions in the small intestine of our bacteria-based IL22 treatment (See Supplementary 1 Fig. S5g). Moreover, no differences were found in IL22 production by ILC3 and *Il22* mRNA in lamina propria cells between mice treated with PBS, *L. reuteri* and *L. reuteri*/IL22 (See Supplementary 1 Fig. S6a, b). *L. reuteri*/IL22 treatment did not affect intestinal indole-3-acetic acid, indole-3-lactic acid and indole-3-aldehyde levels (See Supplementary 1 Fig. S6c-e). Our engineered *L. reuteri* was therefore able to restore intestinal levels of IL22 in mice during chronic–binge ethanol feeding—the bacterially expressed IL22 led to re-expression of REG3G, reduced bacterial translocation, and ethanol-induced steatohepatitis.

No effects of *L. reuteri*/IL22 on liver disease in REG3G-deficient mice

We studied development of liver disease in chronic-binge ethanol-fed *Reg3g*$^{-/-}$ mice gavaged with *L. reuteri*/IL22 or controls, and their wild type littermates. Consistent with our previously published data using a chronic Lieber DeCarli ethanol feeding model for 8 weeks [7], mice deficient for REG3G developed more ethanol-induced liver disease as indicated by increased plasma ALT levels, hepatic triglycerides and inflammation, and bacterial translocation to the liver (Fig. 6a-f). Wild type mice gavaged with *L. reuteri*/IL22 showed ameliorated ethanol-induced liver disease, increased *Reg3g* expression in the small intestine and reduced bacterial translocation to the liver (Fig. 6a-f). We did not observe a reduction in ethanol-induced steatohepatitis in *Reg3g*$^{-/-}$ mice given *L. reuteri*/IL22 (Fig. 6a–c), and hepatic levels of *Cxcl1* mRNAs did not differ significantly in mice fed *L. reuteri*/IL22 vs controls (Fig. 6d). Moreover, equal amounts of bacteria were translocated to the livers of mice fed *L. reuteri*/IL22 vs controls (Fig. 6f). There were no significant differences between groups of mice in liver to body weight ratio, plasma levels of ethanol, or hepatic expression of *Cyp2e1* and *Adh1* mRNAs (See Supplementary 1 Fig. S7a–d). These findings indicate that the protective effect of intestinal IL22 supplementation depends on intestinal REG3G.

Discussion

Changes in genetic, environmental, and dietary factors, as well as alcohol abuse, contribute to intestinal dysbiosis [23, 24]. Nevertheless, the precise mechanism by which alcohol-induced gut dysbiosis causes liver disease are poorly understood. Chronic ethanol feeding reduces expression of REG3G in the small intestine, increasing translocation of bacteria to liver and progression of liver disease [5, 6]. It has not been clear how REG3G expression is downregulated in mice with ethanol-induced liver disease.

We found that ethanol reduces intestinal production of IL22, by altering microbial catabolism of tryptophan into AHR ligands. Restoration of intestinal IL22, by administration of the AHR ligand IAA or via engineered bacteria, reduces ethanol-induced steatohepatitis

by inducing expression of intestinal REG3G, which reduces bacterial translocation to the liver (Fig. 7). Moreover, the reduction in intestinal IAA levels was consistent in patients diagnosed with alcoholic hepatitis compared to healthy controls. These findings indicate the importance of AHR signaling to IL22 to sustain expression of REG3G in the gut during alcoholic liver disease.

Various immune cells produce IL22. Non-lymphoid sources, such as macrophages, neutrophils, and dendritic cells, produce less IL22 compared with lymphoid sources, such as αβ and γδT cells, NK T cells, and ILC [12]. In the intestine, type 3 ILC are a major source of IL22; production depends on cytokines secreted from myeloid cells, mainly IL23 and IL1B [25].

Production of IL22 by ILC is influenced by microbiota [26]. For example, commensal bacteria can suppress intestinal RORγt^+ ILC production of IL22 in healthy mice [27]. In addition, germ-free mice lack expression of *Rorc* and *Il22* mRNAs in the small intestine lamina propria [28, 29]. Commensal bacteria affect ILC populations either indirectly, via recognition by resident myeloid or epithelial cells and subsequent cytokine production, or by direct recognition of commensal bacteria or commensal bacteria-derived products by toll-like receptors, natural cytotoxicity receptors, or the AHR (reviewed in [26]). Indole derivatives from tryptophan catabolism activate the AHR to modulate local IL22 production and regulate intestinal barrier function [14, 16]. Increased AHR signaling inhibits inflammation and colitis in the gastrointestinal tract of mice via production of IL22 [30]. Importantly, the availability and production of AHR ligands from tryptophan is controlled by the microbiota [31]. Metabolomic analyses indicated that germ-free mice have increased levels of tryptophan in plasma and colon, whereas IAA production was impaired in the lumen of the colons [16, 32].

Which microbes produce AHR ligands? Indole derivatives are mostly produced by intestinal bacteria with tryptophanase activity [32]. For instance, lactobacilli activate ILC3 and production of IL22 via their production of AHR ligands, thereby providing epithelial protection while inducing resistance against *Candida albicans* [14]. Interestingly, alcohol-dependent patients have overgrowth of *Candida*, independent of the stage of liver disease [33]. Moreover, dysbiosis in ethanol-fed mice is characterized by reduced *Lactobacillus* [6], whereas several studies demonstrated a beneficial effect of probiotic *Lactobacillus* strains in rodent models of alcoholic liver disease [34, 35]. We found that stimulating lactobacilli using prebiotic fructo-oligosaccharides partially restored expression of REG3G, thereby reducing ethanol-induced steatohepatitis in mice [6]. In the process of tryptophan catabolism, different bacterial enzymes are responsible for the production of indole derivatives. Our current data suggest that certain bacterial strains responsible for specific AHR ligands (i.e. indole-3-lactic acid) were resistant to our antibiotics treatment, thereby potentially restoring intestinal eubiosis and IL22 function. Further studies are needed to identify which bacterial species specifically produce certain AHR ligands, thereby providing more molecular insights and identify new potential targets for therapy.

The ability of systemic IL22 to protect against ethanol-induced liver disease has been described before [21]. Administration of recombinant IL22 or an IL22-expressing

adenovirus during chronic–binge ethanol feeding reduced fatty liver, liver injury, and hepatic oxidative stress, via activation of STAT3 in the liver [21]. We demonstrate that intestine-restricted delivery of IL22 reduces ethanol-induced steatohepatitis by increasing expression of *Reg3g* and preventing bacterial translocation to the liver. These data are in line with our previous findings, in which we show that overexpression of REG3G in intestinal epithelial cells reduces bacterial translocation, and protects mice from ethanol-induced steatohepatitis [7]. In addition to a direct hepato-protective effect of IL22 during ethanol-induced liver disease, IL22 has the beneficial effect of reducing bacterial translocation in intestine.

We have shown that bacteria can be engineered to express specific proteins in the intestine, providing evidence that microbes can be manipulated to act as therapeutic agents. Bacteria that are genetically manipulated to produce specific factors might be more effective than systemic administration of agents, and produce fewer side effects. For example, systemic administration of IL22 increases the risk of liver tumors in patients with chronic liver disease [36, 37, 38]. Studies are needed to determine whether we can increase intestinal AHR signaling with specific AHR ligands, probiotic *Lactobacilli* strains, or bacteria engineered in other ways to reduce progression of alcoholic liver disease. We have identified tryptophan catabolism an important therapeutic target, and offer a strategy to reverse deficiencies in AHR ligands. Increasing the protective functions of the immune responses by these means could lead to new therapeutic strategies.

Methods

Mice

C57BL/6 mice were purchased from Charles River and used in all described experiments. *Reg3g*$^{-/-}$ mice on a C57BL/6 background have been described [39]. Heterozygous mice were used for breeding, and wild type and knockout littermate mice were used in all experiments.

Animal model

Female and male mice (8–12 weeks) were subjected to chronic–binge alcohol feeding (NIAAA) as described previously [9]. Mice were fed with Lieber–DeCarli diet for 15 days, starting at day 6 with ethanol feeding. The caloric intake from ethanol was 0 on days 1–5 and 36% from day 6 until the end. At day 16, mice were gavaged with one dose of ethanol (5 g/kg BW) in the morning and sacrificed 9 hours later. Pair-fed control mice received a diet with an isocaloric substitution of dextrose. Antibiotics treatment was started at day 1 of ethanol feeding, and mice were gavaged daily till harvesting. The composition of antibiotics mixture has been described (Polymyxin B [150 mg/kg BW] and Neomycin [200 mg/kg BW]) [18]. Control mice were gavaged with an equal volume of vehicle (water). Supplementation of IAA was done by daily gavage of 100 μl of 20 mM IAA (initially dissolved in a small volume of NaOH before adjusting with water to prepare the final concentration) or vehicle water, starting at day 1 of ethanol feeding. To study the effect of the engineered bacteria, a volume of 100μl PBS, *L. reuteri* (10^7 CFU/day) or *L. reuteri*/IL22 (10^7 CFU/day) was gavaged daily, starting at day 1 of ethanol feeding. *L. reuteri* and *L. reuteri*/IL22 strains were daily freshly grown in MRS Lactobacilli broth (Sigma), ON at

37°C. All animal studies were reviewed and approved by the Institutional Animal Care and Use Committee of the University of California, San Diego.

Human samples

Non-alcoholic control subjects (n=17; 14 male/ 3 female; mean age = 42) and patients with alcoholic hepatitis (n=13; 9 male, 4 female; mean age = 58; average MELD = 22) were enrolled. Inclusion and exclusion criteria have been described [40]. The protocol was approved by the Ethics Committee of each participating center and patients were enrolled after written informed consent was obtained from each patient. For metabolomics, fecal samples (10mg each) were homogenized using Genogrinder at 1,500rpm for 30s and extracted with 225 μL of - 20°C cold, degassed methanol and 750 μL of methyl tertiary butyl ether (MTBE, Sigma Aldrich, St. Louis, MO). 188 μL of LC-MS grade water was then added to the samples to induce phase separation, followed by centrifugation at 14,000 x g for 2 min. The bottom layer (125 μL) was collected, evaporated to dryness and then resuspended in 60 μL 4:1 acetonitrile and water (v/v) with internal standards. Samples were then vortexed, sonicated for 5 min, centrifuged for 2 min at 14,000 x g and prepared for injection. Hydrophilic interaction liquid chromatography (HILIC) with quadrupole time-of-flight (QTOF) mass spectrometry was used for the untargeted metabolomics profiling as described previously [41]. Briefly, 2 μL of re-suspended sample was injected onto an Acquity UPLC BEH Amide column (150 mm × 2.1 mm; 1.7 μm) coupled to an Acquity VanGuard BEH Amide pre-column (5 mm × 2.1 mm; 1.7 μm, Waters, Milford, MA). The column was maintained at 45°C. Agilent 1290 Infinity UHPLC system (Agilent Technologies, Santa Clara, CA) coupled to a Sciex TripleTOF 5600+ (SCIEX, Framingham, MA, USA) was used. Mobile phase A was 100% LC-MS grade water with 10 mM ammonium formate and 0.125% formic acid (Sigma–Aldrich, St. Louis, MO). Mobile phase B was 95:5 v/v acetonitrile:water (v/v) with 10 mM ammonium formate and 0.125% formic acid (Sigma–Aldrich, St. Louis, MO). Gradient was performed as follows: 0-2 min 100% B, 7.7 min 70% B, 9.5 min 40% B, 10.25 min 30% B, 12.75 min 100% B, isocratic until 16.75 min with a flow rate of 0.4 mL/min. Mass spectra were collected in ESI positive mode with data dependent MS/MS spectra acquisition method. Method blank and human plasma (BioIVT, Westbury, NY) samples were used as quality control samples and injected at the beginning of the run and every ten samples throughout the run. LC-MS raw data files were converted to ABF format and then processed using MS-DIAL version 2.94 [42] for deconvolution, peak detection and alignment. Ion adducts, duplicate peaks and isotopic features were identified using MS-FLO [43]. In house retention time-m/z library and MS/MS spectra databases were used for compound identification. Features present in at least 50% of samples in each group were reported.

Biochemical Assays

Plasma levels of ethanol were measured using the Ethanol Assay Kit (BioVision). Levels of ALT were determined using Infinity ALT kit (Thermo Scientific). Hepatic triglyceride levels were measured using the Triglyceride Liquid Reagents Kit (Pointe Scientific). Levels of IL22 in plasma and culture supernatants were determined using the Mouse IL22 DuoSet ELISA kit according to manufacturer's protocol (DY582, R&D Systems).

Real-time quantitative PCR

RNA was extracted from mouse tissues, and cDNAs were generated [44]. Reverse-transcribed cDNA from tissue or cell culture was amplified on a CFX96 system (Bio-Rad Laboratories) using KAPA SYBR® FAST qPCR Kit Master Mix (2X) (KK4606, Kapa Biosystems) and primers for indicated genes. Primer sequences for mouse genes were obtained from the NIH qPrimerDepot. The qPCR value was normalized to 18S.

Bacterial DNA Isolation and qPCR for 16S

Genomic DNA was isolated from a sterile liver part as previously described [6, 45]. The qPCR value of the 16S rRNA gene [5] was normalized to host 18S rRNA.

Histologic analysis of liver tissues

For determination of lipid content, livers were embedded in O.C.T. compound, sectioned at 7-μm thickness and frozen sections were stained with Oil Red O (Sigma-Aldrich). Samples were analyzed by densitometry, using NIH Image J software. For quantification, the average percentage area positively stained for each mouse was calculated from at least five random pictures of stained liver sections. The results are presented as percentage area positively stained.

Isolation of lamina propria cells

Small intestines were harvested and placed in ice-cold Hank's balanced salt solution (HBSS). After removal of residual mesenteric fat tissue, Peyer's patches were excised and small intestine were opened longitudinally. Tissues were washed in ice-cold HBSS and cut into 1-cm pieces. Then, tissues were incubated in 20 ml of HBSS with 5 mM EDTA, 1 mM sodium pyruvate, 25 mM HEPES and 1 mM dithiothreitol at 37ºC at 150 rpm for 20 minutes. The epithelial cell layer was removed by intensive shaking, washed and stored for further use. After washing in 10 ml of HBSS with 5 mM EDTA, 1 mM sodium pyruvate and 25 mM HEPES, small intestine pieces were minced with scissors and digested in serum-free media containing 1 mg/ml Collagenase (Millipore Sigma), 0.1 U/ml Dispase (Worthington Biochem. Corp., Lakewood, NJ) and 0.1 mg/ml DNase I (Millipore Sigma) at 37ºC at 150 rpm for 30 minutes. Cells were washed and passed through a 70-mm cell strainer. Cells were resuspended in 4 mL of 40% Percoll and placed on 4 mL of 80% Percoll. Percoll gradient separation was performed by centrifugation for 20 minutes at 600 g at room temperature without brake. Lymphoid fractions were collected at the interphase of the Percoll gradient, washed once, and resuspended in fluorescence-activated cell sorter buffer or culture medium.

Flow cytometry

Cells were pelleted, blocked with anti-mouse CD16/32 (1:500, clone 93; 14-0161-85, eBioscience) and stained with CD3-FITC (1:400, 145-2C11, eBioscience). Intracellular cytokine staining was performed using RORγt-PE (1:200, B2D, eBioscience) and IL22-APC (1:100, IL22JOP, eBioscience) antibodies. Intracellular staining was done using the Foxp3/Transcription factor staining buffer set (eBioscience). Cells were recorded using a FACSCanto II flow cytometer. Live single cells were gated using forward scatter (FSC) and

side scatter (SSC), and innate immune cells were identified as T-cells ($CD3^+$) or innate lymphoid cells (CD3-RORγt^+) in which IL22 expression was assessed. Recorded data was analyzed with FlowJo v10 (Treestar Inc.).

HPLC-HRMS analysis

Small intestinal contents were collected by squeezing out the contents using sterile forceps and snap-frozen in liquid nitrogen for storage. Indole derivatives were quantified HPLC-coupled to high resolution mass spectrometry as described before [46].

Engineered *L. reuteri* strain

Plasmid pVPL3524 contains a fusion of a synthetic promoter (P_{RBS1}-SP) and the coding sequence of the murine IL22 gene (NCBI genome accession NO. AC153856.23), the latter codon optimized for expression in *L. reuteri*. Using standard cloning techniques, we replaced the synthetic promoter P_{RBS1}-SP with the *L. reuteri* EF-Tu promoter to yield plasmid pVPL31126. Plasmid pVPL31126 was transformed in *L. reuteri* ATCC PTA 6475 by electroporation to yield *L. reuteri*/IL22 (Laura M. Alexander, Jan Peter van Pijkeren, manuscript in preparation). As control, we transformed *L. reuteri* with pJP028, which is the empty vector control that lacks the gene encoding murine IL22. To test whether *L. reuteri*/IL22 colonizes following 10 days treatment, fecal samples were collected and cultured overnight at 37 degrees on MRS Broth agar plates.

Statistics

All data are displayed as mean ± SEM. For comparison of two groups, the student unpaired t-test was used. For comparison of > 2 groups, one-way analysis of variance (ANOVA) was used followed by Tukey or Fisher's Least Significant Difference (LSD) test. All analyses were performed with GraphPad Prism v7.03. A p-value of < 0.05 was considered significant.

Supplementary Material

Refer to Web version on PubMed Central for supplementary material.

Acknowledgements

This work was supported by an Erwin Schrodinger Fellowship (J4063) from the Austrian Science Fund (to T. Hendrikx), by NIH grants R01 AA020703, R01 AA24726, U01 AA021856, U01 AA026939 (to B. Schnabl), R01 GM124494 (to W. Huang), and by Award Number I01BX002213 from the Biomedical Laboratory Research & Development Service of the VA Office of Research and Development (to B. Schnabl). H. Sokol received funding from the European Research Council (ERC) under the European Union's Horizon 2020 Research and Innovation Programme (ERC-2016-StG-71577). J.P. van Pijkeren was supported by Award Number 233PRJ75PW from the UW-Madison Food Research Institute, and by funds from the UW-Madison Institute of Clinical and Translational Research funded by the National Center for Advancing Translational Science award UL1TR000427.

Abbreviations

AHR	aryl hydrocarbon receptor
ALD	alcoholic liver disease
ALT	alanine transaminase

Europe PMC Funders Author Manuscripts

IAA	indole-3-acetic acid
ILC3	innate lymphoid cell type 3
Reg3	regenerating islet-derived protein 3

References

1. Rehm J, Samokhvalov AV, Shield KD. Global burden of alcoholic liver diseases. J Hepatol. 2013; 59:160–8. [PubMed: 23511777]
2. Szabo G. Gut-liver axis in alcoholic liver disease. Gastroenterology. 2015; 148:30–6. [PubMed: 25447847]
3. Llopis M, Cassard AM, Wrzosek L, Boschat L, Bruneau A, Ferrere G, et al. Intestinal microbiota contributes to individual susceptibility to alcoholic liver disease. Gut. 2016; 65:830–9. [PubMed: 26642859]
4. Mukherjee S, Hooper LV. Antimicrobial defense of the intestine. Immunity. 2015; 42:28–39. [PubMed: 25607457]
5. Hartmann P, Chen P, Wang HJ, Wang L, McCole DF, Brandl K, et al. Deficiency of intestinal mucin-2 ameliorates experimental alcoholic liver disease in mice. Hepatology. 2013; 58:108–19. [PubMed: 23408358]
6. Yan AW, Fouts DE, Brandl J, Starkel P, Torralba M, Schott E, et al. Enteric dysbiosis associated with a mouse model of alcoholic liver disease. Hepatology. 2011; 53:96–105. [PubMed: 21254165]
7. Wang L, Fouts DE, Starkel P, Hartmann P, Chen P, Llorente C, et al. Intestinal REG3 Lectins Protect against Alcoholic Steatohepatitis by Reducing Mucosa-Associated Microbiota and Preventing Bacterial Translocation. Cell Host Microbe. 2016; 19:227–39. [PubMed: 26867181]
8. Sonnenberg GF, Fouser LA, Artis D. Border patrol: regulation of immunity, inflammation and tissue homeostasis at barrier surfaces by IL-22. Nat Immunol. 2011; 12:383–90. [PubMed: 21502992]
9. Bertola A, Mathews S, Ki SH, Wang H, Gao B. Mouse model of chronic and binge ethanol feeding (the NIAAA model). Nat Protoc. 2013; 8:627–37. [PubMed: 23449255]
10. Brandl K, Plitas G, Mihu CN, Ubeda C, Jia T, Fleisher M, et al. Vancomycin-resistant enterococci exploit antibiotic-induced innate immune deficits. Nature. 2008; 455:804–7. [PubMed: 18724361]
11. Vaishnava S, Behrendt CL, Ismail AS, Eckmann L, Hooper LV. Paneth cells directly sense gut commensals and maintain homeostasis at the intestinal host-microbial interface. Proc Natl Acad Sci U S A. 2008; 105:20858–63. [PubMed: 19075245]
12. Parks OB, Pociask DA, Hodzic Z, Kolls JK, Good M. Interleukin-22 Signaling in the Regulation of Intestinal Health and Disease. Front Cell Dev Biol. 2015; 3:85. [PubMed: 26793707]
13. Wolk K, Witte E, Hoffmann U, Doecke WD, Endesfelder S, Asadullah K, et al. IL-22 induces lipopolysaccharide-binding protein in hepatocytes: a potential systemic role of IL-22 in Crohn's disease. J Immunol. 2007; 178:5973–81. [PubMed: 17442982]
14. Zelante T, Iannitti RG, Cunha C, De Luca A, Giovannini G, Pieraccini G, et al. Tryptophan catabolites from microbiota engage aryl hydrocarbon receptor and balance mucosal reactivity via interleukin-22. Immunity. 2013; 39:372–85. [PubMed: 23973224]
15. Lee JS, Cella M, McDonald KG, Garlanda C, Kennedy GD, Nukaya M, et al. AHR drives the development of gut ILC22 cells and postnatal lymphoid tissues via pathways dependent on and independent of Notch. Nat Immunol. 2011; 13:144–51. [PubMed: 22101730]
16. Lamas B, Richard ML, Leducq V, Pham HP, Michel ML, Da Costa G, et al. CARD9 impacts colitis by altering gut microbiota metabolism of tryptophan into aryl hydrocarbon receptor ligands. Nat Med. 2016; 22:598–605. [PubMed: 27158904]
17. Cervantes-Barragan L, Chai JN, Tianero MD, Di Luccia B, Ahern PP, Merriman J, et al. Lactobacillus reuteri induces gut intraepithelial CD4(+)CD8alphaalpha(+) T cells. Science. 2017; 357:806–10. [PubMed: 28775213]
18. Chen P, Starkel P, Turner JR, Ho SB, Schnabl B. Dysbiosis-induced intestinal inflammation activates tumor necrosis factor receptor I and mediates alcoholic liver disease in mice. Hepatology. 2015; 61:883–94. [PubMed: 25251280]

Europe PMC Funders Author Manuscripts

19. Hartmann P, Hochrath K, Horvath A, Chen P, Seebauer CT, Llorente C, et al. Modulation of the intestinal bile acid/farnesoid X receptor/fibroblast growth factor 15 axis improves alcoholic liver disease in mice. Hepatology. 2018; 67:2150–66. [PubMed: 29159825]
20. Holder IA, Boyce ST. Formulation of 'idealized' topical antimicrobial mixtures for use with cultured skin grafts. J Antimicrob Chemother. 1996; 38:457–63. [PubMed: 8889720]
21. Ki SH, Park O, Zheng M, Morales-Ibanez O, Kolls JK, Bataller R, et al. Interleukin-22 treatment ameliorates alcoholic liver injury in a murine model of chronic-binge ethanol feeding: role of signal transducer and activator of transcription 3. Hepatology. 2010; 52:1291–300. [PubMed: 20842630]
22. Xing WW, Zou MJ, Liu S, Xu T, Wang JX, Xu DG. Interleukin-22 protects against acute alcohol-induced hepatotoxicity in mice. Biosci Biotechnol Biochem. 2011; 75:1290–4. [PubMed: 21737938]
23. Starkel P, Leclercq S, de Timary P, Schnabl B. Intestinal dysbiosis and permeability: the yin and yang in alcohol dependence and alcoholic liver disease. Clin Sci (Lond). 2018; 132:199–212. [PubMed: 29352076]
24. Tripathi A, Debelius J, Brenner DA, Karin M, Loomba R, Schnabl B, et al. The gut-liver axis and the intersection with the microbiome. Nat Rev Gastroenterol Hepatol. 2018
25. Rutz S, Wang X, Ouyang W. The IL-20 subfamily of cytokines--from host defence to tissue homeostasis. Nat Rev Immunol. 2014; 14:783–95. [PubMed: 25421700]
26. Sonnenberg GF, Artis D. Innate lymphoid cell interactions with microbiota: implications for intestinal health and disease. Immunity. 2012; 37:601–10. [PubMed: 23084357]
27. Sawa S, Lochner M, Satoh-Takayama N, Dulauroy S, Berard M, Kleinschek M, et al. RORgammat + innate lymphoid cells regulate intestinal homeostasis by integrating negative signals from the symbiotic microbiota. Nat Immunol. 2011; 12:320–6. [PubMed: 21336274]
28. Sanos SL, Bui VL, Mortha A, Oberle K, Heners C, Johner C, et al. RORgammat and commensal microflora are required for the differentiation of mucosal interleukin 22-producing NKp46+ cells. Nat Immunol. 2009; 10:83–91. [PubMed: 19029903]
29. Satoh-Takayama N, Vosshenrich CA, Lesjean-Pottier S, Sawa S, Lochner M, Rattis F, et al. Microbial flora drives interleukin 22 production in intestinal NKp46+ cells that provide innate mucosal immune defense. Immunity. 2008; 29:958–70. [PubMed: 19084435]
30. Monteleone I, Rizzo A, Sarra M, Sica G, Sileri P, Biancone L, et al. Aryl hydrocarbon receptor-induced signals up-regulate IL-22 production and inhibit inflammation in the gastrointestinal tract. Gastroenterology. 2011; 141:237–48. [PubMed: 21600206]
31. Agus A, Planchais J, Sokol H. Gut Microbiota Regulation of Tryptophan Metabolism in Health and Disease. Cell Host Microbe. 2018; 23:716–24. [PubMed: 29902437]
32. Wikoff WR, Anfora AT, Liu J, Schultz PG, Lesley SA, Peters EC, et al. Metabolomics analysis reveals large effects of gut microflora on mammalian blood metabolites. Proc Natl Acad Sci U S A. 2009; 106:3698–703. [PubMed: 19234110]
33. Yang AM, Inamine T, Hochrath K, Chen P, Wang L, Llorente C, et al. Intestinal fungi contribute to development of alcoholic liver disease. J Clin Invest. 2017; 127:2829–41. [PubMed: 28530644]
34. Mutlu E, Keshavarzian A, Engen P, Forsyth CB, Sikaroodi M, Gillevet P. Intestinal dysbiosis: a possible mechanism of alcohol-induced endotoxemia and alcoholic steatohepatitis in rats. Alcohol Clin Exp Res. 2009; 33:1836–46. [PubMed: 19645728]
35. Nanji AA, Khettry U, Sadrzadeh SM. Lactobacillus feeding reduces endotoxemia and severity of experimental alcoholic liver (disease). Proc Soc Exp Biol Med. 1994; 205:243–7. [PubMed: 8171045]
36. Jiang R, Tan Z, Deng L, Chen Y, Xia Y, Gao Y, et al. Interleukin-22 promotes human hepatocellular carcinoma by activation of STAT3. Hepatology. 2011; 54:900–9. [PubMed: 21674558]
37. Park O, Wang H, Weng H, Feigenbaum L, Li H, Yin S, et al. In vivo consequences of liver-specific interleukin-22 expression in mice: Implications for human liver disease progression. Hepatology. 2011; 54:252–61. [PubMed: 21465510]

38. Waidmann O, Kronenberger B, Scheiermann P, Koberle V, Muhl H, Piiper A. Interleukin-22 serum levels are a negative prognostic indicator in patients with hepatocellular carcinoma. Hepatology. 2014; 59:1207. [PubMed: 23729376]

39. Vaishnava S, Yamamoto M, Severson KM, Ruhn KA, Yu X, Koren O, et al. The antibacterial lectin RegIIIgamma promotes the spatial segregation of microbiota and host in the intestine. Science. 2011; 334:255–8. [PubMed: 21998396]

40. Brandl K, Hartmann P, Jih LJ, Pizzo DP, Argemi J, Ventura-Cots M, et al. Dysregulation of serum bile acids and FGF19 in alcoholic hepatitis. J Hepatol. 2018; 69:396–405. [PubMed: 29654817]

41. Showalter MR, Nonnecke EB, Linderholm AL, Cajka T, Sa MR, Lonnerdal B, et al. Obesogenic diets alter metabolism in mice. PLoS One. 2018; 13:e0190632. [PubMed: 29324762]

42. Tsugawa H, Cajka T, Kind T, Ma Y, Higgins B, Ikeda K, et al. MS-DIAL: data-independent MS/MS deconvolution for comprehensive metabolome analysis. Nat Methods. 2015; 12:523–6. [PubMed: 25938372]

43. DeFelice BC, Mehta SS, Samra S, Cajka T, Wancewicz B, Fahrmann JF, et al. Mass Spectral Feature List Optimizer (MS-FLO): A Tool To Minimize False Positive Peak Reports in Untargeted Liquid Chromatography-Mass Spectroscopy (LC-MS) Data Processing. Anal Chem. 2017; 89:3250–5. [PubMed: 28225594]

44. Hartmann P, Haimerl M, Mazagova M, Brenner DA, Schnabl B. Toll-like receptor 2-mediated intestinal injury and enteric tumor necrosis factor receptor I contribute to liver fibrosis in mice. Gastroenterology. 2012; 143:1330–40 e1. [PubMed: 22841787]

45. Fouts DE, Torralba M, Nelson KE, Brenner DA, Schnabl B. Bacterial translocation and changes in the intestinal microbiome in mouse models of liver disease. J Hepatol. 2012; 56:1283–92. [PubMed: 22326468]

46. Miani M, Naour JL, Waeckel-Enée E, Verma Sc, Straube M, Ryffel B, et al. Crosstalk between Gut Microbiota, Innate Lymphoid Cells and Endocrine Cells in the Pancreas Regulates Autoimmune Diabetes. Cell Metabolism. 2018

Europe PMC Funders Author Manuscripts

Europe PMC Funders Author Manuscripts

Summary

What is already known about this subject?

- Alcoholic liver disease (ALD) is characterized by intestinal dysbiosis.
- Chronic ethanol feeding reduces intestinal expression of REG3G in mice and humans.
- REG3G is protective against ethanol-induced liver injury.
- Intestinal *Reg3g* expression is mediated by interleukin-22 (IL22).

What are the new findings?

- Ethanol feeding causes impaired IL22 production by ILC3s in the gut, which is the result of ethanol-induced dysbiosis and lower intestinal levels of indole-3-acetic acid (IAA), a microbiota-dependent AHR ligand.
- Alcoholic hepatitis patients have lower fecal IAA levels compared with healthy controls
- IAA supplementation restores *Il22* and *Reg3g* expression and protects from ethanol-induced steatohepatitis.
- IL22 producing engineered bacteria ameliorate experimental ALD via *Reg3g* induction.

How might it impact on clinical practice in the foreseeable future?

- Engineered IL22-producing bacteria can be used as therapeutics for alcohol-induced liver disease.

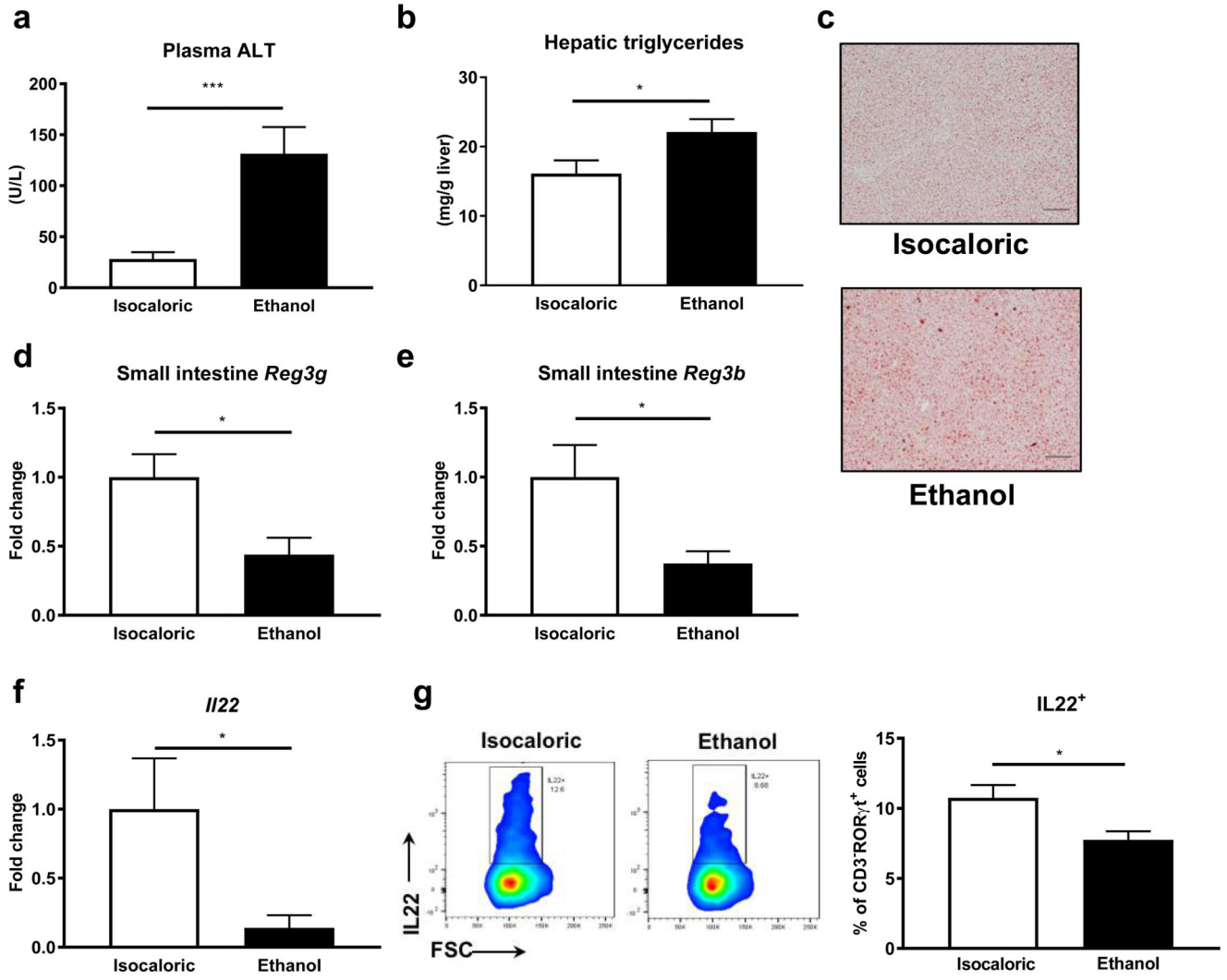

Figure 1. Effects of the chronic–binge ethanol diet.

Plasma levels of ALT (a) and hepatic levels of triglycerides levels (b) in C57BL/6 mice following a control (isocaloric) or chronic–binge ethanol diet. Representative Oil red O staining images of liver tissue (c). Expression of *Reg3g* and *Reg3b* mRNA in jejunum epithelial cells (d, e). Expression of *Il22* mRNA in jejunum lamina propria cells from C57BL/6 mice following a control or chronic–binge ethanol diet (f). Frequencies of IL22-expressing cells in the gated ILC3 population (CD3-RORγt$^+$) after stimulation with IL23 for 4h in jejunum lamina propria cells from C57BL/6 mice after a control or chronic–binge ethanol diet (g). Gene expression levels are shown relative to those of control mice. Data presented are the mean ± SEM of n = 13–15 mice/group. Scale bars = 50 μm. *, *** indicate $p<0.05$, $p<0.001$, respectively.

Europe PMC Funders Author Manuscripts

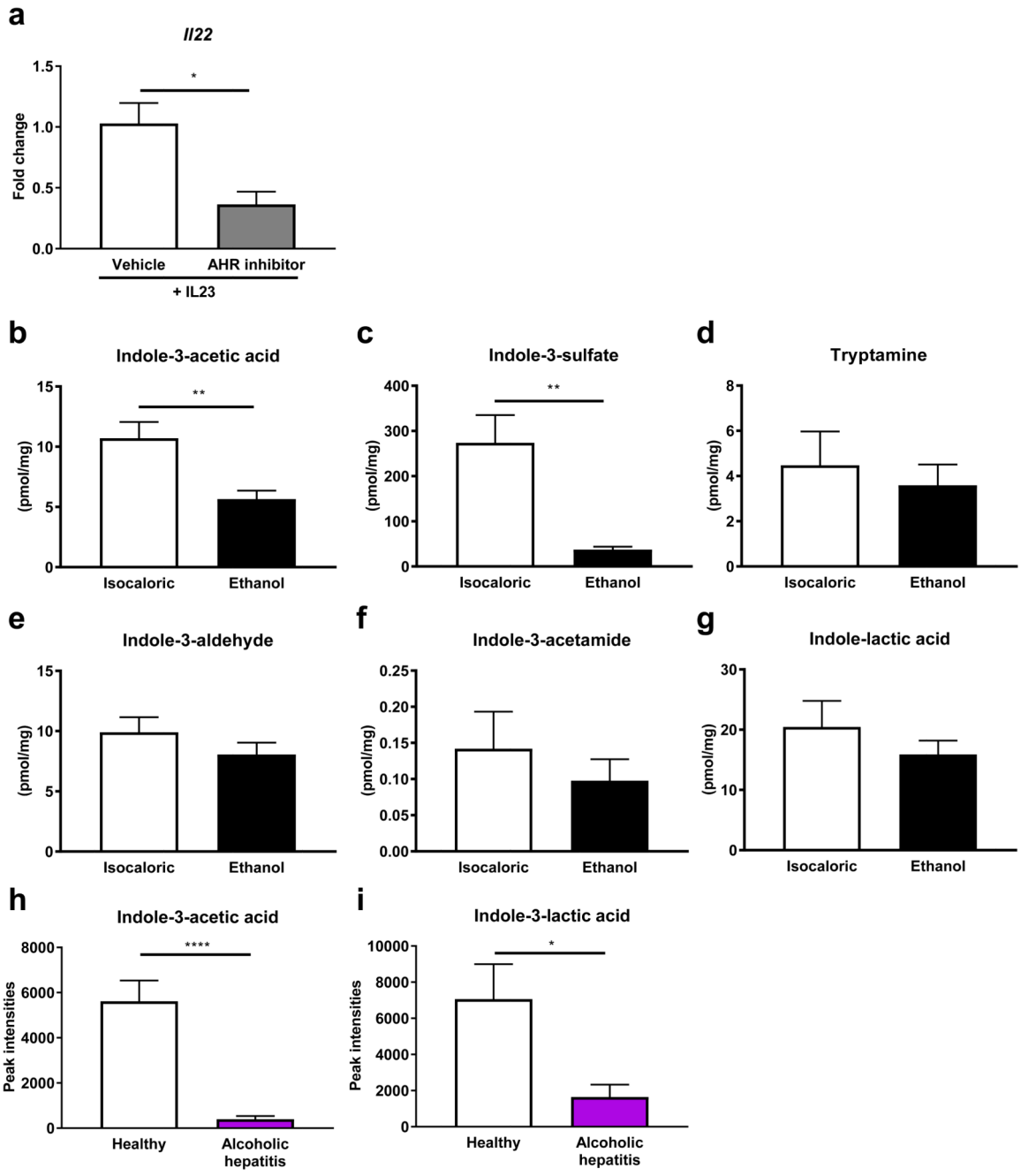

Figure 2. Effects of the ethanol diet on tryptophan metabolism.

Expression of *Il22* mRNA in jejunum lamina propria cells after stimulation with IL23 for 4h, co-incubated with an AHR inhibitor (10 uM CH-223191) or vehicle solution (a). Intestinal levels of indole-3-acetic acid (b), indole-3-sulfate (c), tryptamine (d), indole-3-aldehyde (e), indole-3-acetamide (f), and indole-3-lactic acid (g) of mice fed control (isocaloric) or chronic–binge ethanol diets. Levels of indole-3-acetic acid (h) and indole-3-lactic acid (i) in stool samples of alcoholic hepatitis patients (n=13) and healthy controls (n=17). Gene expression data are set relative to controls (a). Data in all panels are the mean

± SEM of n = 3 biological replicates (a), or n = 10 mice/group (b-f). *, **,**** indicates $p<0.05$, $p<0.01$, $p<0.0001$ respectively.

Europe PMC Funders Author Manuscripts

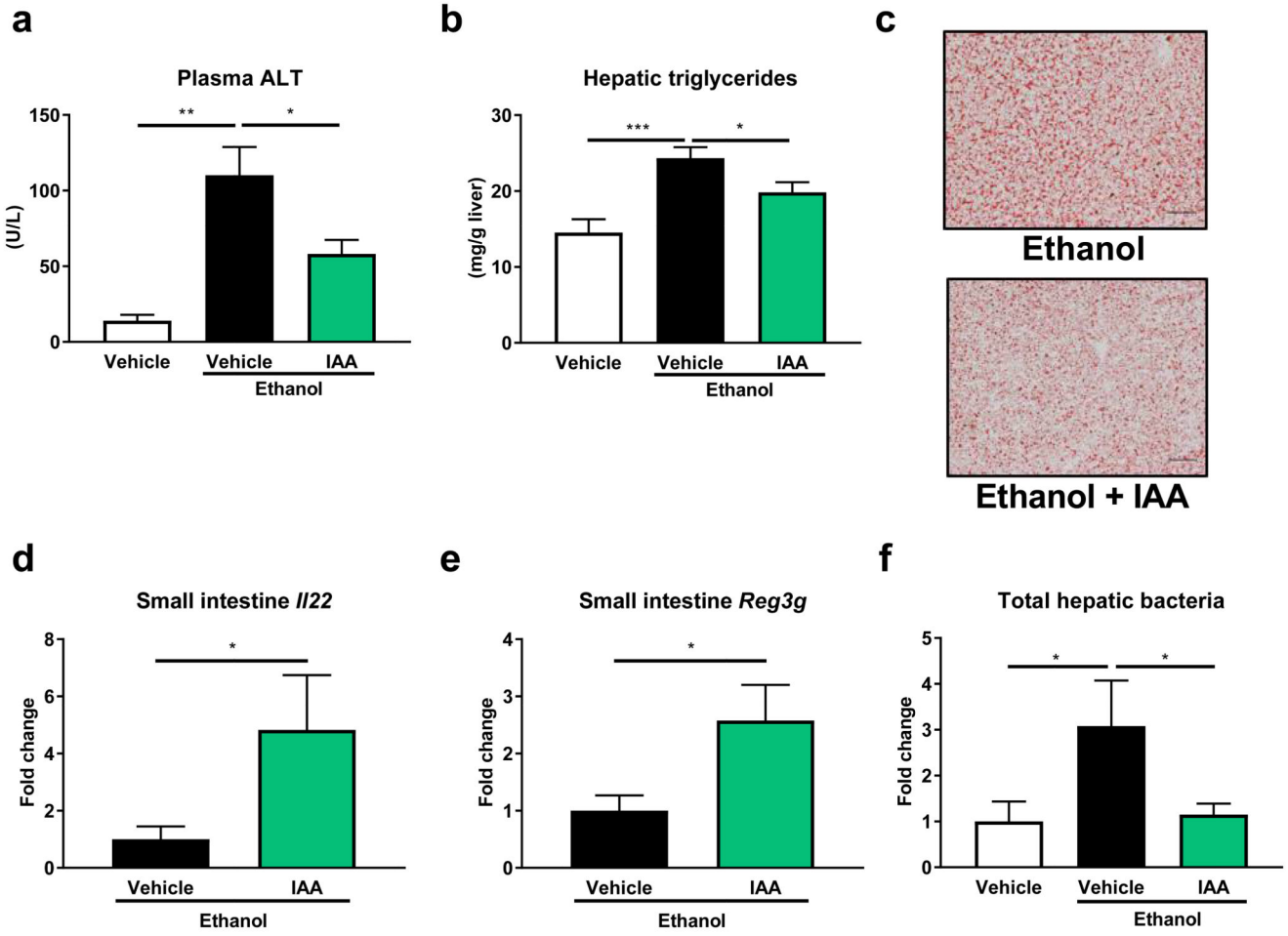

Figure 3. Effects of IAA supplementation.

Plasma levels of ALT (a) and hepatic triglycerides (b) in C57BL/6 mice on a control or chronic–binge ethanol diet, with IAA supplementation (20 mM/day) or vehicle. Representative Oil red O staining images of liver tissue (c). Expression of *Il22* mRNA (d) and *Reg3g* mRNA (e) in ileum of C57BL/6 mice following the chronic–binge alcohol diet, with IAA supplementation or vehicle. Total bacteria in the liver, measured by qPCR for 16S rRNA, normalized to 18S rRNA (f). Gene expression levels are set relative to those of mice given vehicle (d, e). Fold change in hepatic bacteria are compared to mice on the control diet or isocaloric mice (f). Data in all panels are presented as mean ± SEM and are of n = 7 (vehicle/isocaloric), n = 12 (vehicle/ethanol), or n = 14 (IAA/ethanol) mice/group. Scale bars = 50 μm. *, **, *** indicates $p<0.05$, $p<0.01$, $p<0.001$, respectively.

Europe PMC Funders Author Manuscripts

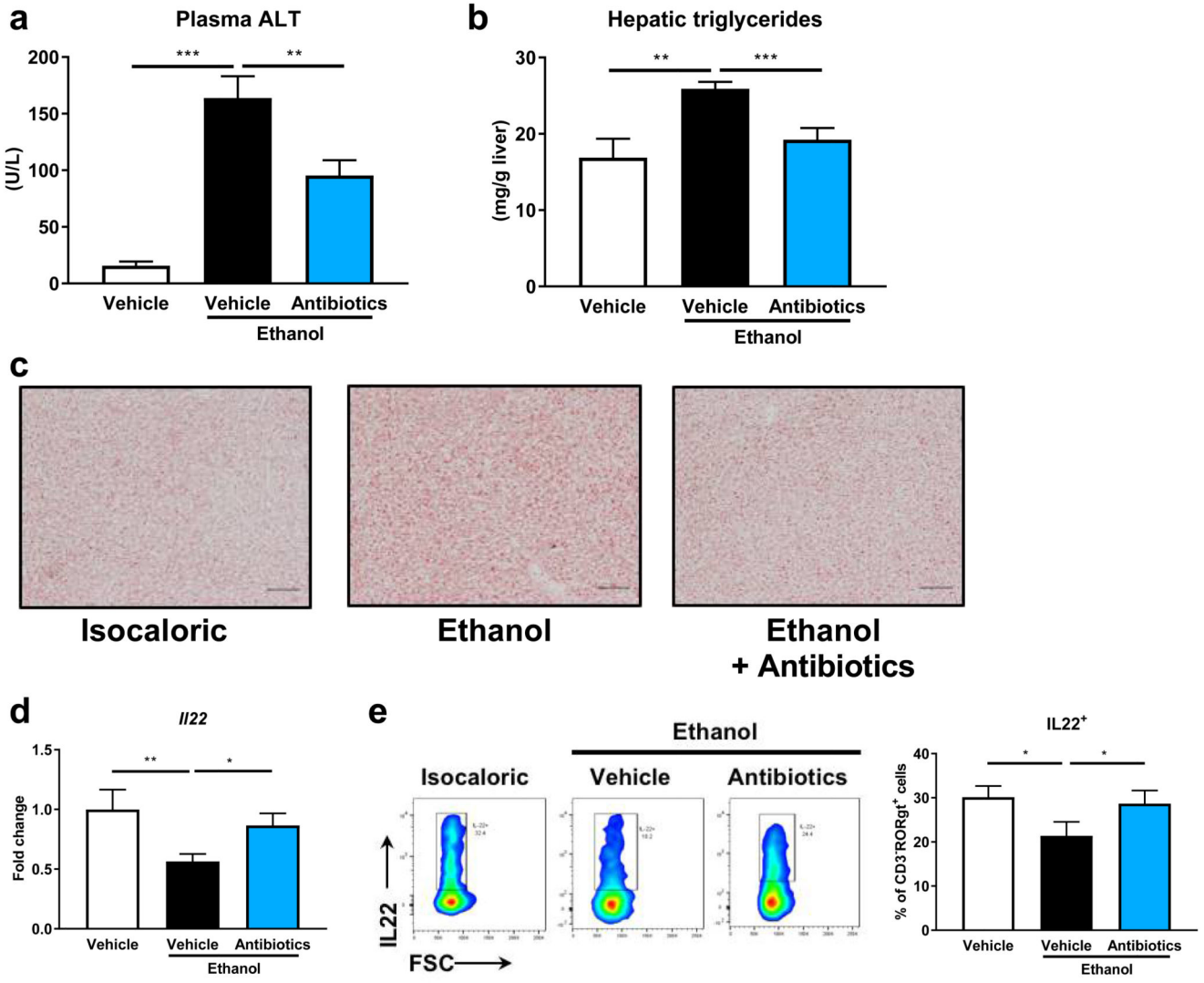

Figure 4. Effects of antibiotics.

Plasma levels of ALT (a) and hepatic triglycerides (b) in C57BL/6 mice on a control (isocaloric) or chronic–binge ethanol diet, with or without antibiotics. Representative Oil red O staining images of liver tissue (c). Levels of *Il22* mRNA in jejunum lamina propria cells from C57BL/6 mice after a control or chronic–binge ethanol diet, with or without antibiotics (d). Frequencies of IL22+ ILC3 (CD3–RORγt^{+}) in jejunum lamina propria of C57BL/6 mice after a control or chronic–binge ethanol diet, with or without antibiotics (e). Gene expression levels are set relative to level of isocaloric-fed control mice. Data presented are the mean ± SEM of n = 10–12 mice/group (a, b) or representative of at least 3 independent stimulations of a minimum of 2 replicates (d, e). Scale bars = 50 μm. *, **,*** indicates $p<0.05$, $p<0.01$, and $p<0.001$, respectively.

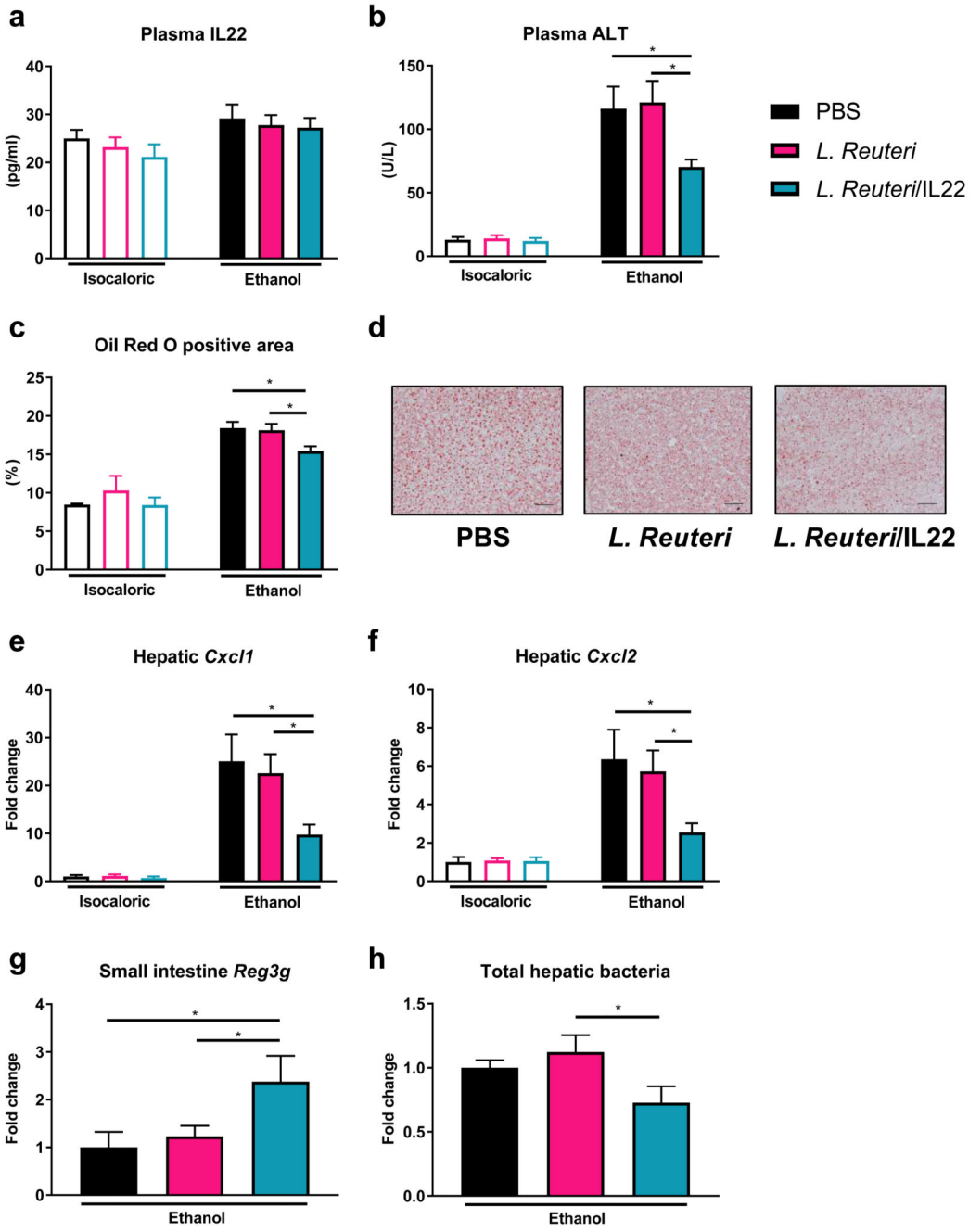

Figure 5. *L. reuteri* engineered to produce IL22 reduce hepatic steatohepatitis and bacterial translocation to the liver.

Plasma levels of IL22 in C57BL/6 mice gavaged with PBS, *L. reuteri*, or *L. reuteri*/IL22 during the control (isocaloric) and chronic–binge ethanol diet (a). Mean plasma level of ALT in these groups of mice (b). Quantification and representative Oil red O staining images of liver tissues from ethanol-fed mice gavaged with PBS, *L. reuteri*, or *L. reuteri*/IL22 (c, d). Hepatic levels of *Cxcl1* mRNA (e) and *Cxcl2* mRNA (f) in mice from these groups. Expression of *Reg3g* mRNA in ileum from mice on the ethanol-diet given PBS, *L. reuteri*, or *L. reuteri*/IL22 (g). Total bacteria in livers of ethanol-fed mice, measured by qPCR for 16S

Europe PMC Funders Author Manuscripts

rRNA, normalized to 18S rRNA (h). Levels are relative to mice given PBS on the control diet (e, f) or mice given PBS while on the ethanol diet (g, h). Data presented as mean ± SEM are of n = 6 (isocaloric groups) and n = 14–16 (ethanol diet) mice/group. Scale bars = 50 μm. * indicates $p<0.05$.

Europe PMC Funders Author Manuscripts

Europe PMC Funders Author Manuscripts

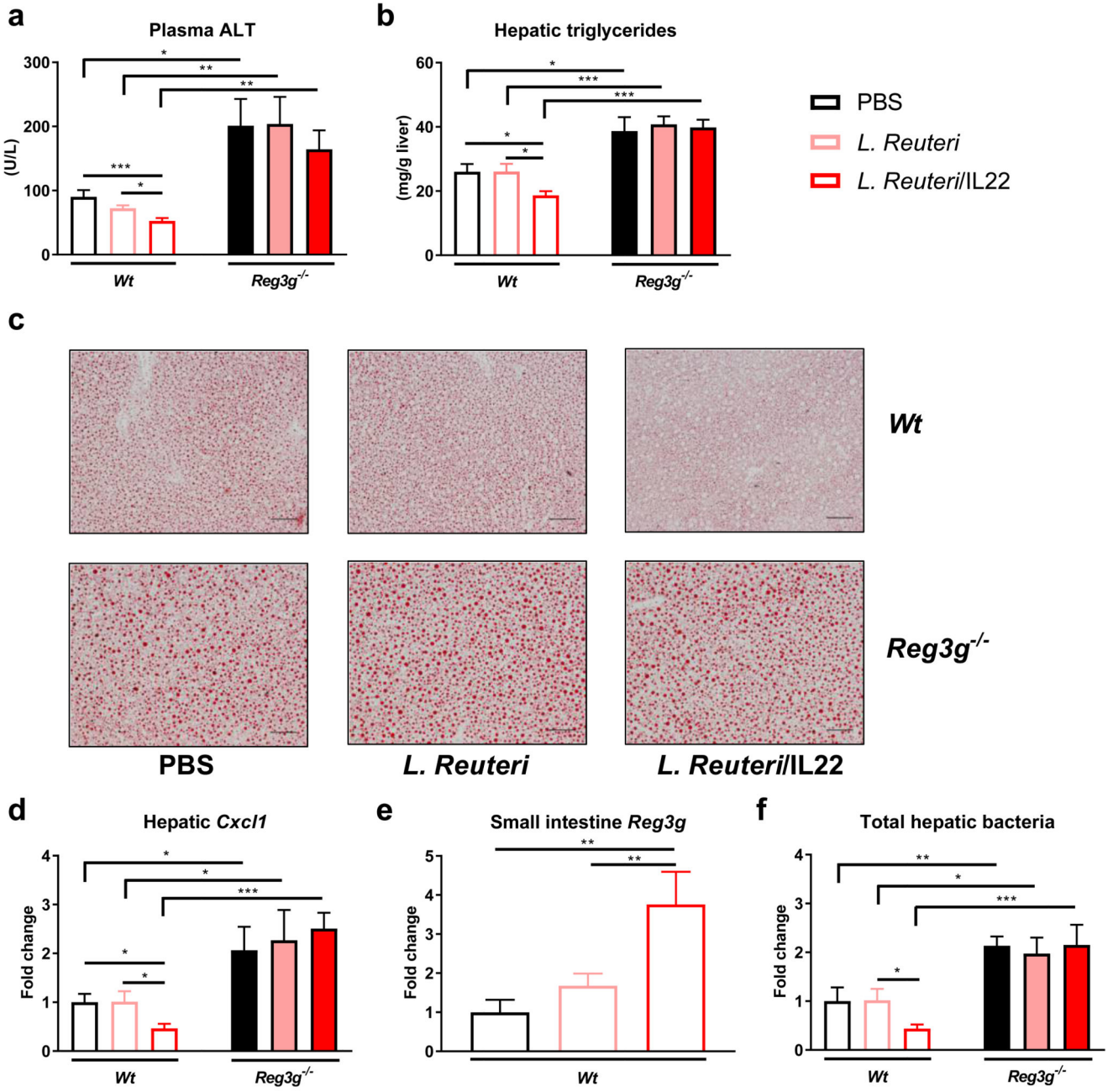

Figure 6. Effects of *L. reuteri*/IL22 in *Reg3g*$^{-/-}$ mice.

Plasma level of ALT in *Reg3g*$^{-/-}$ and wild type (Wt) littermates gavaged with PBS, *L. reuteri*, or *L. reuteri*/IL22 during chronic–binge ethanol diet (a). Hepatic triglycerides and representative Oil red O staining images of liver tissues (b, c). Hepatic expression of *Cxcl1* mRNA (d) in the groups. Expression of *Reg3g* mRNA in ileum from Wt mice on chronic-binge ethanol diet (e). Total bacteria in the liver, measured by qPCR for 16S rRNA and normalized to 18S rRNA (f). Gene expression data are relative to Wt mice given PBS and are presented as mean ± SEM. Experiments performed in n = 51 Wt mice (PBS: 15; *L. reuteri*: 19; *L. reuteri*/IL22: 17) and n = 46 *Reg3g*$^{-/-}$ mice (PBS: 14; *L. reuteri*: 16; *L.*

reuteri/IL22: 16). Scale bars = 50 μm. *, **,*** indicates $p<0.05$, $p<0.01$, and $p<0.001$, respectively.

Europe PMC Funders Author Manuscripts

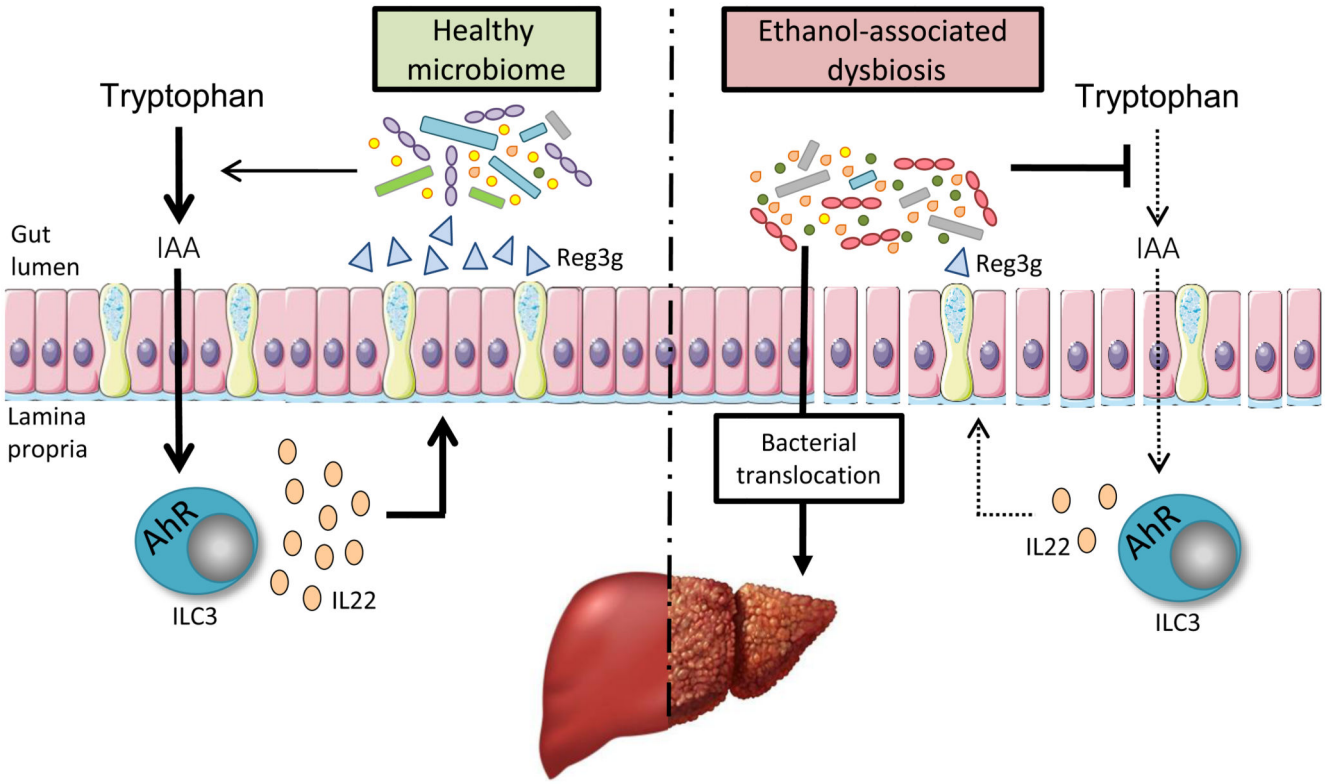

Figure 7. Model for the effects of alcohol on IL22 and REG3G expression.

In healthy conditions, bacterial catabolism of tryptophan into indoles such as IAA promotes AHR-dependent production of IL22 by ILC3s, which maintains expression of REG3G. Chronic alcohol consumption leads to intestinal dysbiosis, which is associated with reduced levels of IAA in the gut. Decreased IAA availability reduces AHR-mediated production of IL22 production by ILC3. This reduces expression of REG3G, allowing bacteria to translocate to the liver, where they promote progression of alcoholic liver disease. (Figure made using Servier Medical Art; http://smart.servier.com)

Europe PMC Funders Author Manuscripts